



Proceedings of the Sixth International Conference on  
Railway Technology: Research, Development and Maintenance  
Edited by: J. Pombo  
Civil-Comp Conferences, Volume 7, Paper 3.15  
Civil-Comp Press, Edinburgh, United Kingdom, 2024  
ISSN: 2753-3239, doi: 10.4203/ccc.7.3.15  
©Civil-Comp Ltd, Edinburgh, UK, 2024

# **Comparative Analysis of Different Models To Estimate the Internal Pressure of a Railway Vehicle Based on Experimental Data**

**F. Moro, C. Somaschini and D. Rocchi**

**Department of Mechanical Engineering, Politecnico di Milano,  
Italy**

## **Abstract**

The estimation of internal pressure in trains is crucial for designing and operating vehicles safely, ensuring both passenger comfort and structural integrity. However, modeling internal pressure presents challenges due to various uncertainties. This study focuses on estimating internal pressure by evaluating different modeling approaches based on experimental measurements conducted on a full-scale train travelling on a track with tunnels presence. To determine the parameters of pressure models efficiently, a rapid and effective method is employed. Modeled internal pressures are then derived using the fitted parameters and experimental external pressures. The comparison of these models against experimental measurements identifies the most suitable internal pressure model for the specific train under consideration and for similar types of vehicles.

**Keywords:** railway vehicles, regional trains, train-tunnel interaction, internal pressure, experimental measurements, pressure models

# 1 Introduction

Aerodynamic phenomena exert significant influence on two critical aspects of vehicle operation: safety and performance. Safety may concern the structural soundness of the vehicle structure (and therefore the passengers' safety too), but also the passengers' comfort (e.g. aural comfort). These effects escalate with the square of the relative speed between the vehicle and the air, becoming particularly noteworthy for trains traveling at speeds exceeding  $100 \text{ km/h}$ . Baker et al. [1, 2, 3] extensively delineate aerodynamic challenges faced by trains, investigative methodologies, and potential remedies for specific issues across various train types, including high-speed (HST), low-speed, and freight vehicles. Notably for HSTs, [4, 5, 6] delve into aerodynamic evaluations for railway structures and rolling stock and propose mitigation strategies. Furthermore, they provide detailed insight into all the others significant aerodynamic phenomena. Numerical tools for aerodynamic issues assessment are extensively used and an overview on them is presented by Hemida [7].

One particular concern is the interaction between trains and tunnels. When a train crosses a tunnel, it generates pressure waves. The complexity amplifies when multiple trains pass through the same tunnel, compounding pressure effects that ultimately impact everything within the tunnel. This can lead to discomfort or, in severe cases, pose safety risks to passengers and compromise the structural integrity of the vehicle. Technical standards address these challenges [8, 9, 10, 11], providing valuable guidance to manufacturers and railway operators. Passengers' comfort and safety concerns are linked to pressure variations within train cars [12, 13]. Standards typically stipulate maximum pressure variation rates for human safety, often associated with aural safety and discomfort. Conversely, structural integrity of the vehicle may be compromised by significant pressure difference between the exterior and interior of the cars. In essence, passengers' safety is assured by minimizing internal pressure fluctuations, while structural safety relies on the minimization of the difference between internal and external pressure variations. Thus, comprehensive knowledge of external and internal pressures is imperative for vehicle design and operational decisions.

Numerous experimental endeavors focus on measuring train pressures within tunnels and assessing the pressure integrity of trains [14, 15, 16, 17, 18, 19, 20]. Some studies attempt to model internal pressures based on external pressures [21, 22], which are typically more readily obtainable through numerical simulations.

This study aims to evaluate the suitability of various internal pressure models, assessing their performance and the associated error in terms of fatigue pressure loads on train structures. These pressure models are applied to experimental data collected from a regional train exhibiting low to medium pressure tightness characteristics. Variations among the models encompass both the physical understanding of internal train car pressures and the mathematical methodologies employed to estimate internal pressures from external inputs. The investigation concludes with a comparative analysis of results and ensuing discussion.

## 2 Method

### 2.1 Experimental data gathering

The foundation of this work lies on experimental measurements conducted on a moving train passing through tunnels. The dataset comprises various experimental campaigns conducted during multiple research activities. The dataset includes:

- Absolute external pressure  $p_{e,i}(t)$  measured on the  $i^{th}$  car in correspondence of one of the doors, outside the vehicle.
- Absolute internal pressure  $p_{i,i}(t)$  measured on the  $i^{th}$  car in correspondence of one of the doors, inside the vehicle.
- Vehicle speed  $v(t)$ .
- Vehicle position  $s(t)$ .

The instrumentation was installed on the first, last, and middle coach of a regional train composed by five coaches, with medium-low pressure tightness.

Due to the rapid variation of outside pressure during tunnel passages, and the different internal pressure dynamics, a pressure difference between the outside and inside of train cars is created (1).

$$\Delta p_i(t) = p_{e,i}(t) - p_{i,i}(t) \quad (1)$$

Pressure measurements were conducted using absolute pressure sensors with sampling frequency of 200 Hz. In order to avoid measurements and turbulence related noise, all the experimental signals are filtered using a low-pass filter with a cut-off frequency of 10 Hz. A total of 25 samples are considered, each of them including the three external and internal pressure time histories.

### 2.2 Internal pressure models

In this work, measured pressure data are available both for internal and external train environments. However, during the design phase or in various other scenarios, it may not be feasible to collect experimental pressures. While there are numerous aerodynamic models for predicting external pressures based on train environment conditions (typically 3D computational fluid dynamics (CFD) codes, but also 1D codes [18, 23]), internal pressure is primarily estimated using mathematical models that rely on external pressure as input [21, 24]. This study examines three internal pressure mathematical models, as detailed in [21]:

- **$\tau$ -model:** adopts a first order differential equation for the estimation of the internal pressure. The time constant is  $\tau$  [s]. Large time constants indicate high pressure tightness of the trains. See Equation 2.

- **$S_{eq}$ -model:** adopts a differential equation based on the equivalent leakage area  $S_{eq}$  [ $m^2$ ]. Small leakage areas indicate high pressure tightness of the trains. In this model parameters like the inside volume of the train  $V$  [ $m^3$ ], the air density  $\rho$  [ $kg/m^3$ ] and the speed of sound  $c$  [ $m/s$ ] are considered. See Equation 3.
- **$Adv$ -model:** (advanced model), adopts a differential equation based both on  $\tau$  and  $S_{eq}$  models. There are two coefficients,  $C_1$  and  $C_2$ , determining the train pressure tightness. This model is a combination of the two aforementioned models. See Equation 4.

All models consider the train structural stiffness through the coefficient  $k$ , acknowledging that pressure changes may result not only from leakages but also from variations in the train's volume under external pressure fluctuations.

$$\frac{dp_{i,i}(t)}{dt} = \frac{k}{k+1} \frac{dp_{e,i}(t)}{dt} + \frac{1}{\tau(k+1)} \Delta p_i(t) \quad (2)$$

$$\frac{dp_{i,i}(t)}{dt} = \frac{k}{k+1} \frac{dp_{e,i}(t)}{dt} + \text{sgn}(\Delta p_i(t)) \frac{c^2 S_{eq}}{V(k+1)} \sqrt{2\rho |\Delta p_i(t)|} \quad (3)$$

$$\frac{dp_{i,i}(t)}{dt} = \frac{k}{k+1} \frac{dp_{e,i}(t)}{dt} + \frac{C_2}{k+1} \Delta p_i(t) + \text{sgn}(\Delta p_i(t)) \frac{C_1}{(k+1)} \sqrt{|\Delta p_i(t)|} \quad (4)$$

Another crucial aspect to consider is the non-uniformity of pressure along the train. It's widely acknowledged that the external pressure experienced by a train passing through a tunnel is not uniform. Consequently, the internal pressure may also exhibit non-uniformity, depending on the connections between the train's cars. To simplify the analysis, external pressures measured on each car are treated as representative of the mean pressure around the car. Internal pressures are handled in two ways, hereon referred as "physical models":

- **Cars pressures:** unique internal pressure for each single cars. Their estimation is based on the external pressures for each car of the train (Figure 1a);
- **Train pressures:** unique internal pressure for the whole train. Its estimation is based on the mean of the external pressures allover the train (Figure 1b).

The choice between these two physical models for internal pressure depends on the train tightness. Pressure-tight trains typically exhibit a uniform internal pressure across all cars, while non-pressure-tight trains are more susceptible to external variations, resulting in internal pressure varying according to the external pressure. Both approaches are employed to model the train's internal pressure, and the determination of the best method will be based on the evaluation indexes described in 2.4.

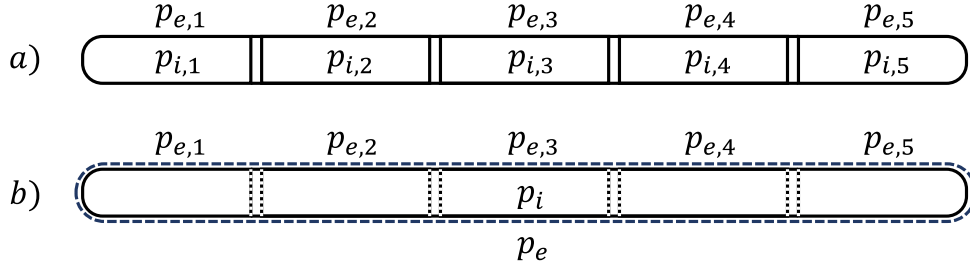


Figure 1: Train internal pressure modelling. a) single cars internal pressure. b) unique internal pressure for all the train.

### 2.3 Experimental pressure fitting method

For each internal pressure model selected, parameters have to be obtained. The internal and external pressures experimental time histories are known and therefore their respective derivatives in time can be easily approximated by finite differences. Equation 2 can be rewritten as

$$Y = a \cdot X_1 + b \cdot X_2 \quad (5)$$

with  $Y = dp_{i,i}/dt$ ,  $X_1 = dp_{e,i}/dt$  and  $X_2 = \Delta p_i(t)$ . The coefficients  $a$  and  $b$  are the unknowns that can be determined by least-squares minimization. Re-arranging the terms  $a$  and  $b$  it is possible to get the model parameters as

$$k = \frac{a}{1 - a} \quad (6a)$$

$$\tau = \frac{1 - a}{b(1 - 2a)}. \quad (6b)$$

In a similar way, Equation 3 can be rewritten as (7) and Equation 4 as (8)

$$Y = a \cdot X_1 + d \cdot X_3 \quad (7)$$

$$Y = a \cdot X_1 + b \cdot X_2 + d \cdot X_3 \quad (8)$$

and the parameters  $S_{eq}$  and  $k$  for the  $S_{eq}$ -model (9) and  $C_1$ ,  $C_2$  and  $k$  for the advanced model (10), are obtained.

$$k = \frac{a}{1 - a} \quad (9a)$$

$$S_{eq} = \frac{dV(1 + k)}{c^2 \sqrt{2\rho}}. \quad (9b)$$

$$k = \frac{a}{1 - a} \quad (10a)$$

$$C_1 = d \cdot (1 + k) \quad (10b)$$

$$C_2 = b \cdot (1 + k). \quad (10c)$$

According to the pressure model adopted, the parameters can be collected and used to estimate the internal pressure starting from the external pressure.

## 2.4 Model comparison method

The primary goal is to establish an internal pressure model that is both mathematically straightforward and accurately reproduces the measured internal pressure. To compare different models and evaluate their ability to provide reliable internal pressure estimates, two distinct approaches are proposed.

Firstly, the comparison is based on the error between the time histories of experimental internal pressure and the modeled pressure derived from the experimental external pressure. This approach focuses on assessing the fidelity of the model to replicate the actual behavior observed in the experimental data.

Secondly, the evaluation incorporates the equivalent pressure difference method defined in the technical norm EN 14067-5[9]. This method is employed to assess the fatigue loads on the train structure resulting from pressure differences between the interior and exterior environments. By comparing the measured equivalent fatigue pressure load with the load predicted by the mathematical model, it becomes possible to determine which model is more or less conservative in terms of structural safety. The methodology involves computing the *rainflow* matrix of the pressure difference, which discretizes the pressure loads based on their amplitude ( $\Delta p_i$ ) and the number of occurrences ( $n_i$ ). Utilizing a general value of  $k = 3$  and assuming an infinite fatigue life number of cycles  $N_c = 10^7$ , the equivalent pressure load  $\Delta p_{eq}$  is derived. It's important to note that this value is intended solely for comparative purposes between different cases and not for assessing strength directly.

$$\Delta p_{eq} = \left( \frac{\sum_i n_i \cdot \Delta p_i^k}{N_c} \right)^{1/k} \quad (11)$$

The mean error method evaluates the proximity of the modeled pressure to the measured pressure, providing insight into the accuracy of the model's predictions. On the other hand, the equivalent pressure error pertains to the accuracy of assessing structural fatigue loading. It is important to recognize that these two indexes serve different purposes. For instance, there may be cases where significant errors in predicting internal pressure do not necessarily translate to significant errors in equivalent pressure load estimation. This highlights the need to consider both error metrics comprehensively, as they offer complementary perspectives on the performance of the models under exam.

$$\bar{e}_p \% = \text{mean} \left( \frac{|p_{i,model} - p_{i,meas}|}{p_{i,meas}} \right) \cdot 100 \quad (12)$$

$$e_{\Delta p_{eq}} \% = \frac{\Delta p_{eq,model} - \Delta p_{eq,meas}}{\Delta p_{eq,meas}} \cdot 100 \quad (13)$$

Depending on the physical modelling adopted, the errors are derived in a slightly different manner. For the *train pressure model*, after the average of the pressure measurement signals over the train, the mathematical parameters are obtained for each

sample, according to the mathematical model adopted. Each sample is then numerically reproduced by the governing differential equation using the respective fitted parameters. The abovementioned errors are computed for every sample and analysed statistically. For the *cars pressure model*, the measurements are not averaged and all the independent cars signals are used to obtain the mathematical parameters. After the numerical reproduction of the samples time histories with the respective parameters, the errors are computed for every car and every sample. At this point the errors are averaged so to have a comparable output with the *train pressure model*.

### 3 Results

The experimental results considered involve the measurements of external and internal pressures for the head, middle and tail cars of the train. In Figure 2 it is represented one of the 25 samples used to fit the internal pressure models. In this specific case the train enters the tunnel at 465 s, and it exits at 490 s.

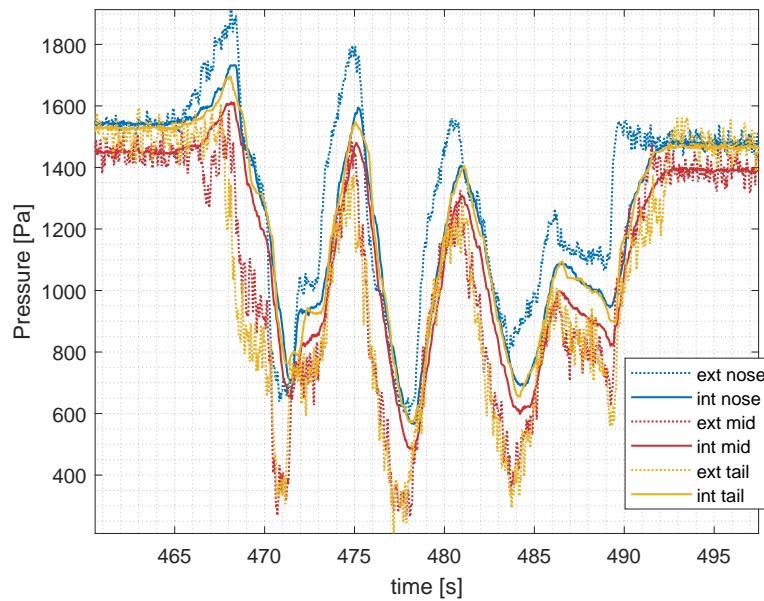


Figure 2: Experimental pressure measurements for the train passing into a tunnel.

Depending on the physical model adopted the results are different. In Figure 3, for the *train pressure model*, the experimental pressures and the modelled internal pressures are reported for the different mathematical models used. The same is depicted in Figure 4 for the case of *car pressure model*, reporting only the data of the first car of the train.

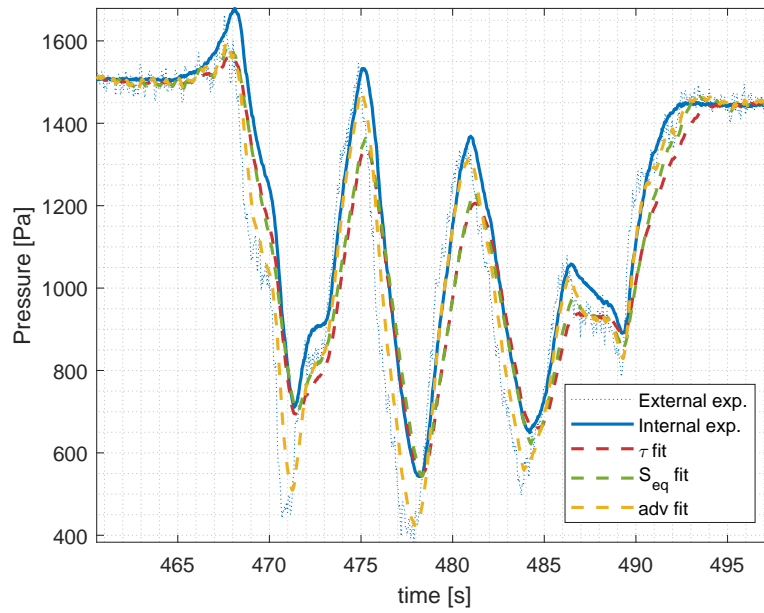


Figure 3: Internal pressure and internal pressure variation fit using different internal pressure mathematical models, train internal pressure.

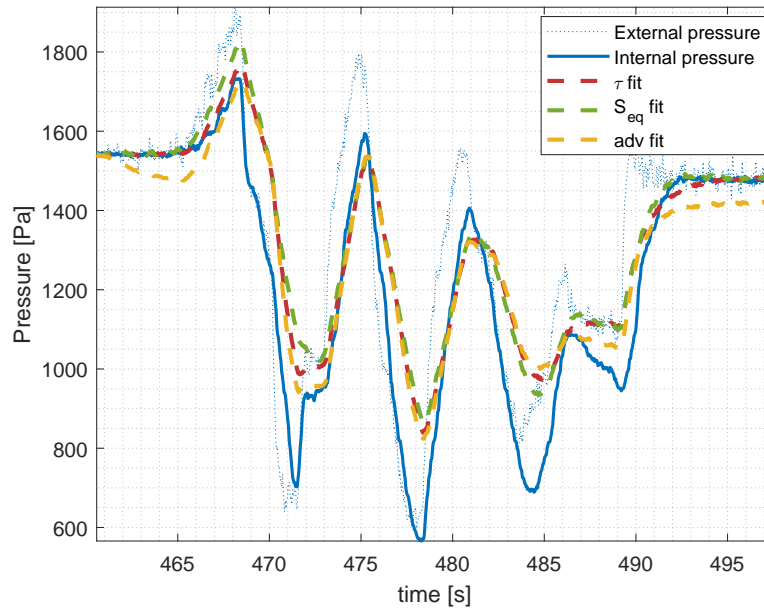


Figure 4: Internal pressure and internal pressure variation fit using different internal pressure mathematical models, cars internal pressure. Nose car data.

Fitting the data with the mathematical models described in 2.3 is represented graphically in Figure 5. The experimental data are approximated by different surfaces depending on the physical model chosen.

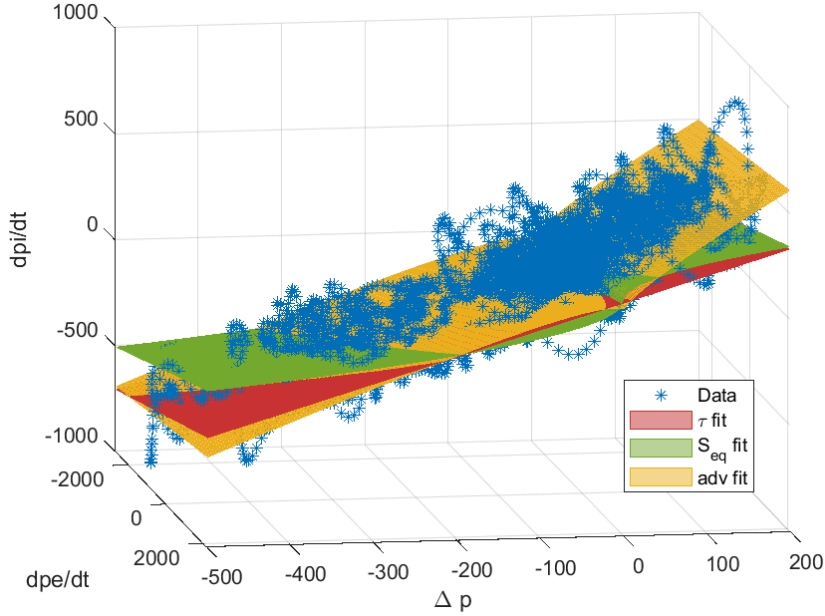


Figure 5: Experimental data fit using different internal pressure mathematical models, train model pressure.

The resulting parameters from the fitting procedure are reported as mean and standard deviation in Table 1 and Table 2.

| $\tau$ -model |                  | $S_{eq}$ -model |                  | $adv$ -model |                  |
|---------------|------------------|-----------------|------------------|--------------|------------------|
| $k$           | [0.0351; 0.0187] | $k$             | [0.0388; 0.0209] | $k$          | [0.0307; 0.0159] |
| $\tau$        | [2.6370; 1.4857] | $S_{eq}$        | [0.0203; 0.0119] | $C_1$        | [3.9735; 4.1437] |
|               |                  |                 |                  | $C_2$        | [1.0478; 0.3650] |

Table 1: Car pressure model, mean and standard deviations  $[\mu; \sigma]$  of parameters.

| $\tau$ -model |                  | $S_{eq}$ -model |                  | $adv$ -model |                  |
|---------------|------------------|-----------------|------------------|--------------|------------------|
| $k$           | [0.0341; 0.0216] | $k$             | [0.0431; 0.0242] | $k$          | [0.0194; 0.0103] |
| $\tau$        | [1.1116; 0.3963] | $S_{eq}$        | [0.0306; 0.0152] | $C_1$        | [8.8464; 7.0878] |
|               |                  |                 |                  | $C_2$        | [1.6107; 0.3947] |

Table 2: Train pressure model, mean and standard deviations  $[\mu; \sigma]$  of parameters.

### 3.1 Models comparison

To assess the accuracy of the pressure model in relation to the measured internal pressure, two indices are employed: the mean error on the internal pressure and the error

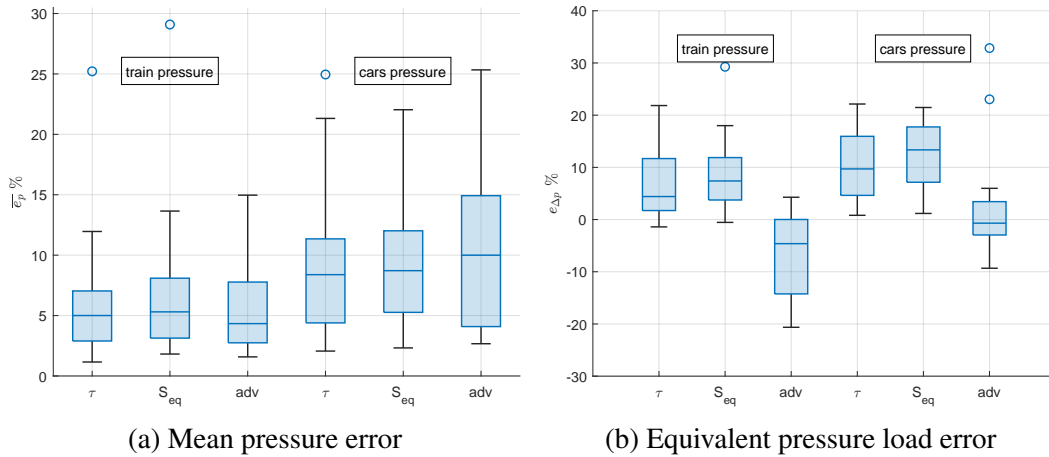


Figure 6: Box plot of error indexes.

in equivalent pressure load. The former evaluates the fidelity of reproducing the experimental internal pressure, while the latter is pertinent for assessing the accuracy of the models in estimating fatigue pressure loads on the train.

The initial decision to make concerns to how the internal pressure is physically modeled, namely using either the "cars pressure" or "train pressure" approach. As previously mentioned, common sense suggests employing the former for trains with low pressure tightness and the latter for trains with high pressure tightness.

Following this, the next consideration is the mathematical model used to derive internal pressure from external pressure, which includes options such as the  $\tau$  model,  $S_{eq}$  model or *advanced model*. Each of these models offers distinct approaches to internal pressure estimation based on external pressure inputs.

Figure 6 shows the results of the different models adopted in terms of errors distribution over the 25 samples available.

## 4 Discussion

To evaluate the models tested, the errors described in Equation 12 and Equation 13 are used. Box plots in Figure 6 give a direct evaluation of the errors collected from all the samples considered. From Figure 6a, it is evident that, based on the mean error, the most effective physical model is the "train pressure model", which assumes a uniform internal pressure for the entire train. Among the mathematical models, the "advanced model" exhibits the lowest mean error. However, as illustrated in Figure 6b, this model underestimates the equivalent pressure load. A similar trend is observed for the "car pressure model". Such underestimation could lead to erroneous design decisions and increased risk of damaging the train structure.

Conversely, the other two mathematical models demonstrate an overestimation of the fatigue equivalent pressure load while maintaining comparable performance to the

”advanced model” in terms of mean error. Furthermore, the straightforward mathematical formulation of the  $\tau$ -model makes it the preferred choice for the train considered in this study.

The values of the parameters reported in Table 2 are consistent with the expected values for a low-medium pressure tight train, proving that the method used for the estimation of such parameters is reliable.

## 5 Conclusions

The evaluation of pressure time histories for a regional train is conducted using the internal pressure fitting method outlined in subsection 2.3. This method has demonstrated efficiency, offering a computationally faster evaluation compared to solving the differential equation directly based on the experimental pressure data and optimizing the model parameters. Instead, the proposed method fits the data directly on the derivatives of the pressures, minimizing the squared error with the experimental data.

The models for internal pressure are categorized into two groups: the physical model, which determines how internal pressure is considered between one car and others on the train, and the mathematical model used to compute internal pressure based on external pressure.

According to the mean error results, the best physical model is the ”train pressure model,” which assumes a uniform internal pressure for the entire train.

Among the mathematical models, the ”advanced” model exhibits the lowest mean error with respect to experimental data. However, it is noted that this model underestimates the equivalent fatigue pressure load. Conversely, the  $\tau$  or  $S_{eq}$  models, while not far from the performance of the advanced model in terms of mean error, provide a margin of safety in pressure load estimation. Specifically, thanks to its easy mathematical formulation, the  $\tau$ -model is the preferred choice for the train considered in this study.

## References

- [1] C. Baker, T. Johnson, D. Flynn, H. Hemida, A. Quinn, D. Soper, and M. Sterling. *Train aerodynamics : fundamentals and applications*.
- [2] C. J. Baker. A review of train aerodynamics Part 1 - Fundamentals, 2014.
- [3] C. J. Baker. A review of train aerodynamics Part 2 - Applications, 2014.
- [4] R. A. Sturt, P. A. Lynch, R. A. Burns, S. A. Clark, B. A. Horton, P. A. Derkowski, A. T. Keylin, and N. T. Wilson. Aerodynamic Assessment and Mitigation – Design Considerations for High-Speed Rail, 2022.

- [5] R. S. Raghunathan, H.-D. Kim, and T. Setoguchi. Aerodynamics of high-speed railway train, 2002.
- [6] S. Srivastava, G. Sivasankar, and G. Dua. A review of research into aerodynamic concepts for high speed trains in tunnels and open air and the air-tightness requirements for passenger comfort. *Proceedings of the Institution of Mechanical Engineers, Part F: Journal of Rail and Rapid Transit*, 236:1011–1025, 10 2022.
- [7] H. Hemida. Contribution of computational wind engineering in train aerodynamics—past and future. *Journal of Wind Engineering and Industrial Aerodynamics*, 234, 3 2023.
- [8] EN 14067-3. Railway applications - Aerodynamics - Part 3: Aerodynamics in tunnels, 2003.
- [9] EN 14067-5. Railway applications - Aerodynamics - Part 5: Requirements and test procedures for aerodynamics in tunnels, 2023.
- [10] Technical specification for interoperability relating to 'safety in railway tunnels' of the rail system of the European Union, 2014.
- [11] Technical specification for interoperability relating to the 'rolling stock — locomotives and passenger rolling stock' subsystem of the rail system in the European Union., 2014.
- [12] R. Gawthorpe. Pressure effects in railway tunnels. 31:P10–P17, 04 2000.
- [13] S. Schwanitz, M. Wittkowski, V. Rolny, and M. Basner. Pressure variations on a train - Where is the threshold to railway passenger discomfort? *Applied Ergonomics*, 44:200–209, 2013.
- [14] T. H. Liu, X. D. Chen, W. hui Li, T. Z. Xie, and Z. W. Chen. Field study on the interior pressure variations in high-speed trains passing through tunnels of different lengths. *Journal of Wind Engineering and Industrial Aerodynamics*, 169:54–66, 10 2017.
- [15] M. Sima, L. Barbone, G. Galeazzo, and P. Gözl. Dynamic Pressure Tightness of Very High Speed Train ETR1000/V300ZEFIRO, 2017.
- [16] D. Rocchi, P. Schito, C. Somaschini, G. Tomasini, T. Argentini, L. Barbone, M. Sima, L. Bocciolini, and G. Galeazzo. Measurement of the aerodynamic features of the ETR1000-V300Zefiro high-speed train, 2017.
- [17] T. Liu, M. Chen, X. Chen, S. Geng, Z. Jiang, and S. Krajnović. Field test measurement of the dynamic tightness performance of high-speed trains and study on its influencing factors. *Measurement: Journal of the International Measurement Confederation*, 138:602–613, 5 2019.

- [18] C. Somaschini, T. Argentini, E. Brambilla, D. Rocchi, P. Schito, and G. Tomasini. Full-Scale Experimental Investigation of the Interaction between Trains and Tunnels. *Applied Sciences*, 10(20), 2020.
- [19] X. Chen, T. Liu, Y. Xia, W. Li, Z. Guo, Z. Jiang, and M. Li. The evolution of airtight performance for a high-speed train during its long-term service. *Measurement: Journal of the International Measurement Confederation*, 177, 2021.
- [20] C. Li, M. Liu, R. Chang, X. Wang, W. Liu, and H. Zhang. Air pressure and comfort study of the high-speed train passing through the subway station. *Sustainable Cities and Society*, 81, 6 2022.
- [21] M. Sima. New unifying procedure for working with pressure tightness of rail passenger vehicles. volume 2, 2003.
- [22] C. J. Chen, Z. Y. He, Y. P. Feng, and L. Yang. Semi-empirical model of internal pressure for a high-speed train under the excitation of tunnel pressure waves. *Proceedings of the Institution of Mechanical Engineers, Part F: Journal of Rail and Rapid Transit*, 236:803–815, 8 2022.
- [23] E. Brambilla, P. Schito, C. Somaschini, and D. Rocchi. Virtual homologation of high-speed trains in railway tunnels: A new iterative numerical approach for train-tunnel pressure signature. *Proceedings of the Institution of Mechanical Engineers, Part F: Journal of Rail and Rapid Transit*, 236:511–531, 5 2022.
- [24] T. Liu, S. Geng, X. Chen, and S. Krajnovic. Numerical analysis on the dynamic airtightness of a railway vehicle passing through tunnels. *Tunnelling and Underground Space Technology*, 97, 3 2020.